

We thank the reviewer for these constructive suggestions.

**Comments 1:**

The authors took most of the paragraphs to describe and calculate the sinking velocities of different coccolith species. However, what is the application of this parameter in future research? This is not very clear to me. I think the purpose of this paper is to give the audience “a refinement of coccolith separation method”. So I suggest adding some paragraph to introduce how to use your SV data in routine work or to give the audience some suggestions how to improve the efficiency or precision of the separation method after your work.

**Reply:** In this study, we indeed focused on the measurement of coccolith sinking speeds. We do not try to propose a new protocol for coccolith separation, instead our empirical data can be used to refine settling time choices using existing protocols. Once sinking velocities are estimated for coccoliths in a particular sample set, coccoliths can be separated by the protocols described in Bolton et al. (2012) or Stoll and Ziveri (2002), using optimal settling times, vessels, and concentrations from this study. We have added a brief descriptions of separation protocol (Lines 247-272).

**Comments 2:**

In this manuscript, the authors used several technique and methods in the experiments, such as “sinking method or filtering method” in L83 or “drop technique” in L99. This would be difficult to follow for the audience who are not very familiar with coccolith separation. I suggest adding some brief explanations of these techniques.

**Reply:** Thank you for this suggestion. We have added a brief description of the micro-filtering method in Lines 41-43. The description of sinking/decanting method can be found in the Line 49-53. For the drop technique, we have rewritten chapter 2.2.2 and added more details about this method (Lines 101-119).

**Comments 3:**

The authors selected eight raw sediment samples from different cores in global oceans. As I know, these cores have different geographic settings like different water depths, mineral composition and nannofossil preservation. Do these factors influence the separation process or the sinking velocity?

**Reply:** Yes, these factors may influence the separation process. We have included a short discussion of the potential influence of dissolution on sinking velocity in Lines 233-235 (Lines 206-207 in former version). But we do not discuss the influence of thickness on coccolith sinking velocity, which will be an interesting point for future study. As for the mineral composition, we suggeste that if the content of suspension is below a certain level, the clay or quartz or any other mineral particles can be ignored in hindering settling (similar question was also answered in [Reply](#) to Review 1’s **Comments 1**).

**Comments 4:**

The section of “Conclusions”, this part is more or less like a part of discussion and not so constructive to me. I suggest improving this part.

**Reply:** We have rewritten this part as ‘Conclusion and suggestion for separation’. See the new version.

**Comments 5:**

In L86-87, “except the *Pseudoemiliana lacunosa* and *Umbilicosphaera sibogae*, which cannot be separated from each other”. Why? Should give some explanations.

**Reply:** The only reason is they have similar sinking velocities. We have explained this in our new 'Conclusion and suggestion for separation' section.

**Comments 6:**

In L188-189, "If we use data for all species except *Helicosphaera carteri*. . ." why don't include *H. carteri* in the calibration?

**Reply:** Thanks for pointing out that this needs clarification. We didn't use *H. carteri* in the regression because of its specific shape, which is quite different to the other species studied. This was explained in Lines 224-233 (Lines 203-205 in the former version): the ellipticity of *H. carteri* (~0.6) is significant lower than other coccolith (among 0.8-0.9), therefore its settling behavior differs from other species. This is also illustrated in Figure 6d and Figure C3. We have reorganized this part to make it clearer.

**Comments 7:**

L66, change "two Neogene samples" to "two Neogene/Paleogene samples"

**Reply:** Done.

**References**

Bolton, C.T., Stoll, H.M., Mendez-Vicente, A., 2012. Vital effects in coccolith calcite: Cenozoic climate-pCO<sub>2</sub>drove the diversity of carbon acquisition strategies in coccolithophores, *Paleoceanography* 27, doi:10.1029/2012pa002339.

Stoll, H.M., Ziveri, P., 2002. Separation of monospecific and restricted coccolith assemblages from sediments using differential settling velocity. *Marine Micropaleontology* 46, 209-221, doi: 10.1016/S0377-8398(02)00040-3.

## 1 A refinement of coccolith separation methods: Measuring the sinking 2 characters of coccoliths

3 Hongrui Zhang<sup>1,2</sup>, Heather Stoll<sup>2</sup>, Clara Bolton<sup>3</sup>, Xiaobo Jin<sup>1</sup>, Chuanlian Liu<sup>1</sup>

4 <sup>1</sup> State Key Laboratory of Marine Geology, Tongji University, Shanghai, 200092, China

5 <sup>2</sup> Geological Institute, Department of Earth Science, Sonneggstrasse 5, ETH, 8092, Zürich, Switzerland

6 <sup>3</sup> Aix-Marseille Univ, CNRS, IRD, Coll de France, CEREGE, Aix en Provence, France.

7 Correspondence to: Chuanlian Liu ([liucl@tongji.edu.cn](mailto:liucl@tongji.edu.cn))

8 **Abstract.** ~~The Quantification~~ sinking velocities of individual coccoliths ~~are relevant~~ will contribute  
9 ~~to for export of their CaCO<sub>3</sub> from the surface ocean, and for optimizing~~ laboratory methods ~~to for~~  
10 ~~separating~~ coccoliths of different sizes and species for geochemical analysis. ~~In the laboratory,~~ †The  
11 repeat settling/decanting method was the earliest method ~~proposed~~ to separate coccoliths from  
12 sediments ~~for geochemical analyses~~, and is still widely used. However, in the absence of estimates  
13 of settling velocity for non-spherical coccoliths, previous implementations have depended mainly  
14 on time consuming empirical method development by trial and error. In this study, the sinking  
15 velocities of coccoliths belonging to different species were carefully measured in a series of settling  
16 experiments for the first time. Settling velocities of modern coccoliths range from 0.154 to 10.67  
17 cm h<sup>-1</sup>. We found that a quadratic relationship between coccolith length and sinking velocity fits  
18 well and coccolith sinking velocity can be estimated by measuring the coccolith length and using  
19 the length-velocity factor,  $k_{sv}$ . We found a negligible difference in sinking velocities measured in  
20 different vessels. However, an appropriate choice of vessel must be made to avoid ‘hindered settling’  
21 in coccolith separations. The experimental data and theoretical calculations presented here ~~will~~  
22 support and improve the repeat settling/decanting method.

## 23 1. Introduction

24 Coccolithophores are some of the most important phytoplankton in the ocean. They can secrete  
25 calcareous plates called coccoliths, which contribute significantly to discrete particulate inorganic  
26 carbon in the euphotic zone and to CaCO<sub>3</sub> fluxes to the deep ocean (e.g., Young and Ziveri, 2000;  
27 Sprengel et al., 2002), ~~and~~ Coccolith morphology, geochemistry and fossil assemblage  
28 composition can reflect record paleoenvironmental changes (e.g., Beaufort et al., 1997; Stoll et al.,  
29 2002; Zhang et al., 2016). However, the use of coccolith geochemical analyses in  
30 paleoenvironmental reconstructions ~~is~~ was so far hindered by the difficulty of isolating coccolith  
31 compared with foraminifera. Two main methods have been developed to concentrate near-  
32 monospecific assemblages of coccoliths from bulk sediments: one is the method based on a  
33 decanting technique (Paull and Thierstein, 1987; Stoll and Ziveri, 2002) and the other is that based  
34 on microfiltration (Minoletti et al., ~~2008~~2009). The improvement of separation techniques offered  
35 a new perspective to study the Earth's history (e.g. Stoll, 2005; Beltran et al., 2007; Bolton and Stoll,  
36 2013; Rousselle et al., 2013). Moreover, the development of coccolith oxygen and carbon isotope  
37 studies in culture in recent years (e.g. Ziveri et al., 2003; Rickaby et al., 2010; Hermoso et al., 2016;  
38 McClelland et al., 2017) has provided an improved mechanistic understanding of coccolith isotope  
39 data and therefore stimulated the need for more purified coccolith fraction samples from the fossil  
40 record.

41 Both decanting and microfiltering are widely used methods for coccolith separation. The  
42 Microfiltering method separates coccoliths with polycarbonate micro-filter membrane ~~relies~~  
43 ~~heavily on the specifications of micro filter membrane (such as with pore sizes of 2µm, 3µm, 5µm~~  
44 ~~and 8µm, 10µm and 12µm pore size), and~~ This method is highly effective in the larger size ranges,  
45 but is very time consuming in sediments with a high proportion of ~~very~~ small (<5µm) coccoliths  
46 (which tends to be the case in natural populations). It is also impossible to separate coccoliths with  
47 similar lengths by microfiltration, such as *Florisphaera profunda* and *Emiliania huxleyi* (Hermoso  
48 et al., 2015). Decanting, on the other hand, is highly effective for the small-sized coccoliths, because  
49 their slow settling times permit a greater ability to separate different sizes. Consequently, in some  
50 studies, a combination of the micro filtering and sinking or centrifugation method were applied for  
51 coccolith separation (Stoll, 2005; Bolton et al., 2012; Hermoso et al., 2015). The repeated

52 sinking/decanting method, first employed by (Edwards, 1963; Paull and Thierstein, 1987) follows  
53 the simple principle formalized by Stokes' Law for spherical particles: particles of larger size settle  
54 more quickly because they have a higher ratio of volume and mass (accelerating sinking) to sectional  
55 area (resistance retarding sinking). However, the sinking velocities of coccoliths with complex  
56 shape are difficult to calculate and have not been quantified in previous studies. Consequently, the  
57 repeated decanting method has generally used settling times based on empirical trial and error.

58 In ~~this~~ the current study, we present a novel and rigorous estimation of ~~the~~ sinking velocity for 16  
59 species of modern and Cenozoic coccoliths, carefully measured in 0.2% ammonia at 20°C. With this  
60 new dataset, we explore how to estimate the sinking velocity of coccoliths based on their shape  
61 and length, which allows our estimations to be generalized for other species, and for situations where  
62 the mean thickness-length of coccoliths of a given species was different from that of our study.  
63 These generalizations, together with our results on sinking velocities of one coccolith species  
64 (*Gephyrocapsa oceanica*) in different vessels, should allow a significant improvement in efficiency  
65 of future protocols for separation of coccoliths by repeated decanting.

## 66 2. Materials and methods

### 67 2.1 Sample selections

68 We measured the sinking velocity of 16 different species of coccoliths, ~~isolated from eight deep-~~  
69 ~~sea sediment samples from the Pacific and Atlantic Oceans (Figure 1, Table A1). Sample were~~  
70 ~~principally of Quaternary age but including~~ two Neogene/Paleogene samples ~~(Figure 1).~~  
71 In general, nNumbers of small coccoliths, including *E. huxleyi*, *Gephyrocapsa* spp and  
72 *Reticulofenestra* spp. are about an order of magnitude greater than that of larger coccoliths. However,  
73 the larger coccoliths' contributions to carbonate can be as high as 50% (Baumann, 2004; Jin et al.,  
74 2016). Moreover, both small coccoliths and large coccoliths are useful in geochemical analyses  
75 (Ziveri et al., 2003; Rickaby et al., 2010; Candelier et al., 2013; Bolton et al., 2012, 2016; Bolton  
76 and Stoll, 2013). Therefore, both small and large coccoliths were studied in this research. ~~The~~  
77 ~~coccoliths were isolated from eight samples from the Pacific and Atlantic Oceans (more location~~  
78 ~~information are in Figure 1 and Table A1; the pictures of studied coccolith can be found in Appendix~~  
79 ~~B). All Pictures of the studied coccolith are shown in Appendix B, and all classifications of coccolith~~

80 follow Nannotax3 except *Reticulofenestra* spp. (Figure C2 in Appendix C).

## 81 2.2 Experiment designs

### 82 2.2.1 Sample pretreatments

83 The sinking velocity measurement depends on absolute abundance estimation (more details in 2.2.2).  
84 However, on microscope slides, larger coccoliths and foraminifer fragments may cover smaller  
85 coccoliths, reducing the accuracy of coccolith absolute numbers. Thus, before sinking experiments  
86 were carried out, raw sediments were pretreated to purify the target coccoliths to reduce errors in  
87 coccolith counting. The raw sediments were disaggregated in 0.2% ammonia and sieved through a  
88 63 µm sieve and then treated by sinking method or filtering method (Bolton et al., 2012; Minoletti  
89 et al., ~~2008~~2009) to concentrate the target species up to at least more than 50% of the total  
90 assemblages (for Noëlaerhabdaceae coccoliths, a percentage more than 90% can be easily achieved).  
91 In one sample with aggregation (ODP 807), we did a rapid settling (30 min, 2 cm) to eliminate  
92 aggregates. Most of the species were measured individually in settling experiments, except ~~the for~~  
93 *Pseudoemiliana lacunosa* and *Umbilicosphaera sibogae*, which ~~cannot be separated from each~~  
94 ~~other~~were measured together.

### 95 2.2.2 Measuring the sinking speeds of coccoliths

96 We are not aware of any prior direct determination of the sinking velocity of individual coccoliths,  
97 although the sinking velocities of live coccolithophores and other marine ~~algae~~ algal cells have been  
98 successfully measured by the 'FlowCAM' method (Bach et al., 2012) or a similar photography  
99 technique (e.g. Miklasz and Denny, 2010). Here we introduce a simple method to measure the  
100 particle sinking speeds without special equipment.

101 1. After pretreatment, the coccolith suspensions were gently shaken and then moved into  
102 comparison tubes which were vertically mounted on tube shelves. We set the timer going  
103 and let the suspension settle for a specified period of time, marked as sinking time or  
104 settling duration (T);—

105 2. Thereafter, we removed the upper 15 ml supernatant into a 50 ml centrifuge tube with a 10  
106 ml pipette. This operation ~~should be~~ was, performed slowly and gently to avoid drawing  
107 lower suspensions upward. The absolute counting of coccolith was achieved by using the  
108 'drop technique' to make quantitative microscope slides (Koch and Young, 2007; Bordiga

Formatted: Font color: Text 1

Formatted: List Paragraph, Numbered + Level: 1 +  
Numbering Style: 1, 2, 3, ... + Start at: 1 + Alignment:  
Left + Aligned at: 0.63 cm + Indent at: 1.27 cm

Formatted: Font color: Text 1

Formatted: Font color: Text 1

et al., 2015). 0.3 ml mixed suspension was extracted and pipettes onto a glass cover and dry the slider on a hotplate;

3. The lower suspension was than to homogenized and another slider was prepare as described above;

4. The number of coccoliths in the upper and lower suspensions were carefully counted by the 'drop technique' on microscope at  $\times 1250$  magnification and the number of coccoliths and fields of view (FOV) were recorded for further calculations, which is a quick method to determine absolute abundance of coccoliths (Koeh and Young, 2007; Bordiga et al., 2015). More than 300 specimens were counted for most of the measurements. For the *Helicosphaera carteri* measurements, more than 100 FOV were checked and about 100 specimens were counted.

To calculate the sinking velocities of coccoliths, we define a parameter named the separation ratio (R), which represents the percentage of removed coccoliths in one separation by pumping out the upper suspension. This parameter is important and will be repeatedly mentioned in the following part. R was measured using the following equation (more details about derivation can be found in Appendix D):

$$R = \frac{\frac{N_1}{n_1} \times V_1 V_2}{\frac{N_1}{n_1} \times V_1 V_2 + \frac{N_2}{n_2} \times V_2 V_2} \quad (2-1)$$

where  $N_1$  and  $N_2$  are numbers of coccoliths counted in upper and lower suspension slides, respectively;  $n_1$  and  $n_2$  are the number of fields of view (FOV) counted.  $V_1$  and  $V_2$  are the volume of the settling vessel defined by the settling distance, as shown in Figure 2.

The separation ratio, R, also has a relationship with sinking time, T (Appendix D):

$$R = \frac{V_1 - \frac{V_1}{D} \times sv \times T}{V_1 + V_2} \quad (2-2)$$

where  $V_1$ ,  $V_2$  and D are shape parameters shown in Figure 2; and  $sv$  is the average sinking velocity of measured coccoliths. If we plot R against T, the slope of line has a relationship with  $sv$ . Hence Then liner regressions between R and T were processed with MATLAB to calculate the  $sv$  (details about error analyses can be found in Appendix E).

There are still two issues to be explained. The first one Firstly, is to eliminate the shape differences among vessels, all separation ratios have been transferred to calibrated separation ratios ( $R_{cal}$ ), which means the separation ratio measured in a standard vessel with  $V_1=15$  ml,  $V_2=10$  ml and  $D=6$  cm

Formatted: Font color: Text 1

Formatted: Font color: Text 1

Formatted: Font: Italic

Formatted: Font color: Text 1

Formatted: Subscript

Formatted: Subscript

Formatted: Subscript

Formatted: Subscript

Formatted: Subscript

Formatted: Subscript

Formatted: Subscript

Formatted: Subscript

Formatted: Subscript

Formatted: Subscript

Formatted: Subscript

138 (more details [about transformation from R to R<sub>cal</sub> can be found](#) in Appendix D). ~~The other one is~~  
 139 ~~that~~ [Secondly](#), we treated the average sinking velocities as the sinking velocities of the coccoliths  
 140 with the average length. This approximation has been proved reasonable in Appendix D.

### 141 2.2.3 Detecting the potential influence of vessels

142 Seven commonly used vessels were selected to detect the potential influence of vessels (Figure 3).  
 143 Two of them are made of plastics (No.2 and No.3 in Figure 3) and all others are pyrex glass vessels.  
 144 About 500 mg of sediment from ~~the~~-core KX21-2 were pretreated as described in 2.2.1 and  
 145 suspended in about 500 ml ammonia. After that, settling experiments were performed as described  
 146 in 2.2.2 using different vessels. In these experiments, only the dominant species, *G. oceanica*, was  
 147 measured.

### 148 2.2.4 Other factors influencing the sinking velocity

149 Temperature can change the density and viscosity of liquid. Generally speaking, the higher the  
 150 temperature is, the lower the density and viscosity will become and the faster pellets will sink. Take  
 151 water for instance, if the temperature increases from 15 to 30°C, the particle sinking velocity will  
 152 increase by ~43% (Table 1). All sinking velocities measured or discussed in the following sections  
 153 were velocities at 20°C to minimize the influence of temperature.

154 The calibration of sinking velocity in high concentration suspension has been calculated by  
 155 Richardson and Zaki (1954)

$$156 \quad sv = sv_0(1 - \alpha_s)^{2.7} \quad (2-3)$$

157 where the  $\alpha_s$  is the solids volume fraction. Based on equation 2-3, the higher the suspension  
 158 concentration is, the slower the sinking velocity will be. That is so called 'hindered settling'. When  
 159 the  $\alpha_s=0.2\%$ , the reduction of sinking velocity owing to hindered settling ~~is negligible cannot be~~  
 160 ~~neglectable~~-( $sv/sv_0$  equals 99.46%). Hence, in this study all suspensions have solid volume fractions  
 161 lower than 0.2% to avoid notable reductions of coccolith sinking velocities.

## 162 3. Results and Discussions

### 163 3.1 Influence of vessels

164 The sinking velocities of *G. oceanica* in the core KX21-2 in 0.2% ammonia at 20°C measured in  
 165 different vessels vary from 0.99 to 1.23 cm h<sup>-1</sup>. The lowest value occurred in the 100 ml centrifuge



166 tube and the highest sinking velocity was measured in the 50 ml centrifuge tube experiments. The  
167 correlations between sinking velocities and different vessel parameters are quite low:  $r=0.13$  for the  
168 vessel inner diameter,  $r=0.0005$  for the sinking distance and  $r=0.051$  for the upper volume and total  
169 volume ratio ( $V_1/(V_1+V_2)$ ). The dissipation of energy by friction between the moving fluid and the  
170 walls can cause a reduction of sinking speed (wall effect). A significant wall effect will be detected  
171 when a particle is settling in a vessel ~~which with a diameter~~ that is smaller than the particle size by  
172 two orders of magnitude (Barnea and Mizarchi, 1973). The length of coccoliths is on the micron  
173 scales, so the diameters of vessel used in laboratory are ~~about~~ more than ~~three-four~~ orders  
174 magnitude larger than coccoliths. Moreover, our results show that the difference between vessel  
175 materials, glass and plastics, can also be ignored (Figure 4). Hence, we suggest that vessel type  
176 almost has no significant influence on sinking velocity of coccoliths.

177 However, our experiments were premised on the basis that the concentration of suspension was  
178 equal among different vessels. This means that large vessels can treat more sediment at one time but  
179 if we choose a larger vessel, more suspensions should be pumped and it often costs more time in  
180 sinking (often due to longer sinking distance). Assuming that the sediment is composed of 50%  
181 calcite (with density of  $2.7 \text{ g cm}^{-3}$ ) and 50% clay (about  $1.7 \text{ g cm}^{-3}$ ), the largest amount of sediment  
182 that can be used without significant reduction of the sinking velocity (5%) is about 400 mg in 100  
183 ml suspension (this calculation is based on equation 2-3). However, ~~because the~~ sediments  
184 ~~accumulating~~ accumulate in the lower suspension, the particle concentration can be more than 4  
185 times higher than in the initial homogenous concentration. This phenomenon will be more  
186 significant for a vessel with a narrow bottom, such as centrifuge tubes. To avoid this, we recommend  
187 using about 100 mg dry sediment ~~should be~~ suspended in at least 100 ml suspension to avoid  
188 ‘hindered settling’. If more sediment is necessary for geochemistry analyses, then a larger vessel  
189 should be selected to separate enough sample ~~in~~ at one time.

Formatted: Subscript

Formatted: Subscript

Formatted: Subscript

### 190 3.2 Sinking velocities at 20°C in 0.2% ammonia

191 We measured the separation ratios of different coccoliths in comparison tubes at 20°C in 0.2%  
192 ammonia (Figure 5). The sinking velocities of coccoliths were then calculated by linear fitting of  
193 separation ratios and settling durations. The sinking velocities of studied coccoliths vary by ~~one-two~~  
194 orders of magnitude from  $0.154 \text{ cm h}^{-1}$  to  $10.67 \text{ cm h}^{-1}$  (Table 2). The highest sinking velocity was

195 found in the measurement of *Coccolithus pelagicus* and the lowest velocity was found for *F.*  
196 *profunda*. The average sinking speeds of coccoliths is about 10-50% of the terminal sinking  
197 velocities of calcite spheres calculated by Stokes' Law (Figure 6c). These ratios are comparable with  
198 ~~the~~ to the oval objects (e.g. seeds) data from Xie and Zhang (2001) and smaller than steel ellipsoids  
199 ~~these data~~ from McNown and Malaika (1950). The sinking velocities of coccoliths measured in our  
200 experiment are about 2-3 orders of magnitude smaller than values from sediment traps of 143-243  
201 m d<sup>-1</sup> (595~1012 cm h<sup>-1</sup>) in the North Atlantic (Ziveri et al., 2000 and Stoll et al., 2007), confirming  
202 suggesting the fact that the coccoliths sinking out of the euphotic layer are mainly in the form of  
203 sinking aggregates rather than individual coccoliths.

### 204 3.3 Estimating the sinking velocities

205 Generally speaking, the sinking velocities of coccoliths increase with ~~the~~ distal shield length (Figure  
206 5a), as expected from the increase in volume to sectional area for a given geometry as length  
207 increases. Our data implies that the sinking velocity has a power function relationship with distal  
208 shield length.

209 We propose that the sinking velocity of coccoliths might have a quadratic relationship with distal  
210 shield length as described by Stokes' Law (Figure 6a). If we use data for all species except  
211 *Helicosphaera-H. carteri* (the reason can be found in the following discussion), the sinking  
212 velocities can be described by the following equation:

$$213 \quad sv = 0.0982 (\pm 0.001) * \phi^2 \quad (3-1)$$

214 Based on this quadratic regression, we derive a shape-velocity factor ( $k_{sv}$ ) that relates settling  
215 velocity to coccolith length.

$$216 \quad sv = k_{sv} * \phi^2 \quad (3-2)$$

217 Furthermore, this factor is analogous to the shape-mass factor, ' $k_s$ ' used to relate coccolith mass to  
218 coccolith length (Young and Ziveri, 2000). The length and shape-velocity factor of coccoliths can  
219 be used to predict most of the sinking velocity variations, however, variations may also arise due to  
220 changes in coccolith mass and thickness, for a given length, and due to the hydrodynamics of  
221 particular shapes. We noticed that the smaller coccolith *G. caribbeanica* has a greater sinking  
222 velocity than the larger coccolith, *G. oceanica*. We suggest that this was caused by greater mass per  
223 length (or greater average thickness) in the case of *G. caribbeanica* and this may be due to the closed

224 central area while *G. oceanica* has an open central area. Another example is *H. carteri*, ~~its which~~  
225 ~~lower~~~~smaller~~ sinking velocity ~~of which~~ can be explained by the unique structure ~~of~~ *H. carteri*  
226 ~~coccolith~~. ~~Firstly~~, the broad edge of *H. carteri* can increase the drag force significantly, ~~and~~ *H.*  
227 *carteri* has the largest ellipticity (major axis length and minor axis length ratio) among the measured  
228 coccoliths, which means the mass of *H. carteri* is smaller than other species of coccoliths with  
229 similar lengths (Figure 6d and Figure C3). Moreover, most of the measured coccoliths have a  
230 ellipticity (major axis length and minor axis length ratio) larger than 0.8, while the ellipticity of *H.*  
231 *carteri* is around 0.6, which means the mass of *H. carteri* is smaller than other species of coccoliths  
232 with similar lengths (Figure 6d and Figure C3). That is also the reason *H. carteri* was excluded from  
233 the general regression in equation 3-1. In the case of partial dissolution, the well-preserved  
234 *Cyclicargolithus floridanus* may have higher mass than dissolved (or disarticulated) *Cy. floridanus*,  
235 and therefore a slightly higher shape-velocity factor.

#### 236 **4. ~~Conclusions~~ Suggestions for coccolith velocity estimations and separations**

237 To improve coccolith separation by settling methods, we measured sinking velocities of different  
238 coccoliths by gravity. Sinking velocities in this study varied from 0.154 to 10.61 cm h<sup>-1</sup>, about 10%  
239 to 50% of those of calcite spheres with same diameter. The shape of different vessels had little  
240 impact on the sinking velocity. But we should consider the volume of vessels to avoid 'hindered  
241 settling'. The sinking velocities are mainly controlled by the shape of coccolith, including the distal  
242 shield length, the size of central area, and the ellipticity of coccoliths. Besides the shape of coccoliths,  
243 temperature is also crucial to the coccolith separations because of the dependence of sinking  
244 velocities on temperature. Length-velocity factors were proposed to estimate coccoliths sinking  
245 velocities, so coccolith ~~sinking speeds in different samples can be easily estimated~~ separation can be  
246 achieved by following steps:

- 247 1) Measure the ~~mean~~ length ~~of~~ coccoliths in your target assemblage under the  
248 microscope and regress the length distribution by the assumption of normal distribution  
249 (details are in Appendix C);
- 250 2) Estimate sinking velocities for each important species. For species which ~~sinking~~  
251 speed has been directly measured, we can use the length-velocity factor directly ( $v = k_v * \phi^2$ ).  
252 For unmeasured species, we can choose the length-velocity factor of coccoliths

Formatted: Font: Italic

Formatted: Font: Italic

Formatted: Font: Not Italic

Formatted: Numbered + Level: 1 + Numbering Style: 1, 2, 3, ... + Start at: 1 + Alignment: Left + Aligned at: 1.27 cm + Indent at: 1.9 cm

253 with similar morphology in this study or use the general length-velocity formula  
254 ( $v=0.098(\pm 0.001)*\phi^2$ );

255 3) Calculate the separation time for main species. For example, in KX21-2 there are three  
256 main coccoliths, *F. prounda*, *G. oceanica* and *Ca. leptoporus* and we wish to separate  
257 *G. oceanica* out from the bulk sediment. Calculate each coccoliths' sinking velocity  
258 distributions as described in Step 2 above. As shown in Figure 7, a sinking velocity  
259 intermediate between *F. profunda* (with a length  $2\sigma$  larger than average, marked as  $+2\sigma$ )  
260 and *G. oceanica* (with a length  $2\sigma$  smaller than average, marked as  $-2\sigma$ ) optimal to  
261 separate them, would be  $0.6\text{ cm h}^{-1}$ . Similarly, we can chose speed thresholds  $1.85\text{ cm}$   
262  $\text{h}^{-1}$  to separate *G. oceanica* from *Ca. leptoporus*. If we settle in a 50 ml centrifuge tube  
263 with a sinking distance, D, equal to 5.84 cm, the sinking time for separating *F. profunda*  
264 should be  $T=5.84/0.6=9.73\text{ h}$ . Similarly, we can calculate the time for separating *G.*  
265 *oceanica* by  $T=5.84/1.85=3.16\text{ h}$ :

266 4) Homogenize the sediment suspension and let coccoliths settling as the period  
267 calculated in Step 3. After that, pump out the upper part of suspension. In the upper  
268 part, we have exclusively the smaller of the main coccoliths. However, column will  
269 still contain some smaller ones. So this step (settling and pumping) should be repeated  
270 until the lower part no longer has significant contribution from the smaller coccoliths.  
271 This step has been well described in pervious studies and more details can be found in  
272 Stoll and Ziveri (2002) and Bolton et al. (2012).

273 We find, iif we use the general formula, it should be noted that a closed central area coccolith will  
274 sink faster than prediction (for *G. caribbeanica* and small *Ca. leptoporus* will settle ~40% faster)  
275 and coccoliths with greater ellipticity can settle much slower (for *H. carteri* will settle as 30% of  
276 the predicted sinking velocity for coccolith with similar length). Moreover, the sinking method  
277 cannot separate every species of coccoliths perfectly. As mentioned in Section 2.2.1, *P. lacunosa*  
278 and *U. sibogae* cannot easily be separated from each other because they have similar sinking  
279 velocities. Nevertheless, this study provides the first direct estimation of coccolith settling velocities,  
280 which should simplify implementation of future methods to separate coccoliths by settling time.

281

Formatted: Font: Italic

Formatted: Font: Italic

Formatted: Font: Italic

Formatted: Font: Italic

Formatted: Font: Italic

Formatted: Superscript

Formatted: Font: Italic

Formatted: Font: Italic

Formatted: Font: Italic

Formatted: Font: Italic

Formatted: Font: Italic

Formatted: Font: Italic

282 *Acknowledgements.* This study was supported by grants from the Chinese National Science  
283 Foundation (91428310, 91428309 and 41530964, to L.C.). We thank the Integrated Ocean Drilling  
284 Program (IODP) for providing the samples. The IODP is sponsored by the U.S. National Science  
285 Foundation and participating countries under management of the IODP Management International,  
286 Inc (IODP-MI).

287 **Table 1.** The influence of temperature on sinking velocity. Density data is from Kell (1975) and  
 288 viscosity data is from Joseph et al. (1978).

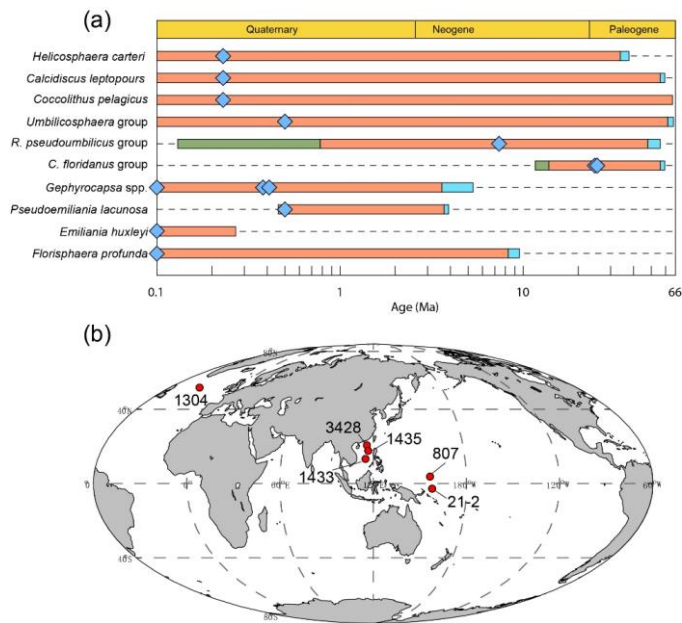
T (°C)	$\rho$ (g cm <sup>-3</sup> )	$\eta$ (mPa s)	$SV_{VT} : SV_{VT=20}$
15	0.9991	1.1447	0.8804
20	0.9982	1.0087	1
25	0.9970	0.8949	1.1279
30	0.9956	0.8000	1.2627

289 **Table 2.** The sinking velocity and shape-velocity factor of different coccolith species:  $\phi$  means the  
 290 distal shield length of coccolith and St  $\phi$  is the standard deviation of distal shield length; sv represents  
 291 the sinking velocity;  $sv_{95\%-}$  (95%-) and  $sv_{95\%+}$  (95%+) represent the lower and higher limit of 95%  
 292 confidence level, respectively. 'k<sub>sv</sub>' represents the length-sinking velocity factor. The short name of  
 293 coccolith can be found in the caption of Figure 4. The details of coccoliths length distribution are in  
 294 Appendix C.

Species	abb.	$\phi$ ( $\mu$ m)	St $\phi$ ( $\mu$ m)	sinking velocity (cm h <sup>-1</sup> )	$sv_{95\%-}$ (95% -)	$sv_{95\%+}$ (95% +)	k <sub>sv</sub>
<i>F. profunda</i>	Fp-WP	1.508	0.557	0.158	0.010	0.011	0.070
<i>F. profunda</i>	Fp-SCS	1.786	0.641	0.154	0.051	0.052	0.048
small <i>Reticulofenestra</i>	Ret (<4um)	2.454	0.509	0.848	0.354	0.416	0.141
<i>E. huxleyi</i>	Emi	2.512	0.469	0.853	0.054	0.064	0.135
<i>Gephyocapsa</i> spp.	G spp	2.755	0.502	0.752	0.125	0.147	0.099
<i>G. caribbeanica</i>	Gcar	3.312	0.352	1.873	0.174	0.192	0.171
<i>U. sibogae</i>	Umb	4.060	0.500	1.268	0.416	0.441	0.077
<i>G. oceanica</i>	Geo	4.187	0.517	1.170	0.155	0.178	0.067
<i>P. lacunosa</i>	Pla	4.350	0.617	1.171	0.337	0.338	0.062
Small <i>Ca. leptoporus</i>	Cal small	4.605	0.629	3.351	0.172	0.199	0.158
large <i>Reticulofenestra</i>	Ret(>4um)	4.988	0.605	2.379	0.534	0.641	0.096
<i>Cy. floridanus</i>	Cyf	5.805	0.963	4.174	0.320	0.336	0.124
(dissolved) <i>Cy. floridanus</i>	Cyf -d	6.134	0.727	4.508	0.352	0.417	0.120
Large <i>Ca. leptoporus</i>	Cal large	6.370	0.931	3.737	1.053	1.336	0.092
<i>H. carteri</i>	Hel	8.936	0.994	2.541	1.740	2.440	0.032
<i>Co. pelagicus</i>	Cpl	10.640	1.175	10.610	0.950	1.235	0.094

295

296 **Figure 1.** Temporal and spatial distribution of samples. (a) The evolution of studied coccoliths: first  
 297 occurrence and last occurrence data are from Nannotax3  
 298 (<http://www.mikrotax.org/Nannotax3/index.html>). The blue bars represent ranges of first occurrence  
 299 and the green bars represent ranges of last occurrence. The blue diamonds represent samples used in  
 300 this study. (b) Spatial distribution of samples. 1304 means IODP U1304, 3428 means MD12-3428cq,  
 301 1433 and 1435 means IODP U1433 and U1435, respectively. 807 means ODP 807 and 21-2 means  
 302 KX21-2.

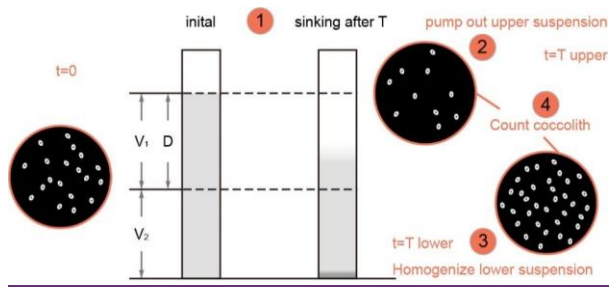


303

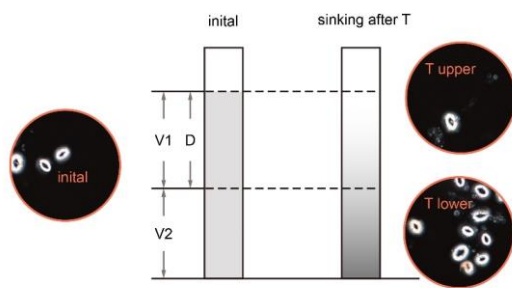
304

305 **Figure 2.** Schematic of settling experiments. ~~The pictures were taken after *Coccolithus pelagicus*~~  
306 ~~sinking experiments with  $T=0$  and  $T=30$  min.~~  $V_1$  and  $V_2$  are the volumes of the upper and lower  
307 cylinders,  $D$  is the settled distance. ~~The numbers in circles are same as the number of Steps described in~~  
308 ~~Section 2.2.1.~~

309



310

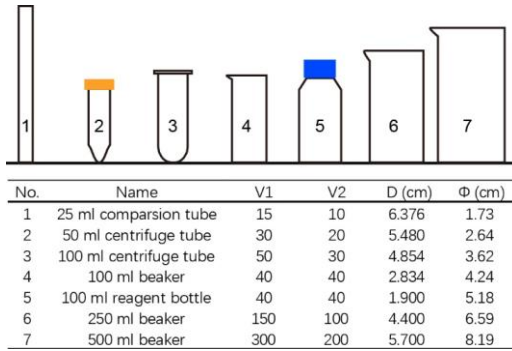


Formatted: Subscript  
Formatted: Subscript



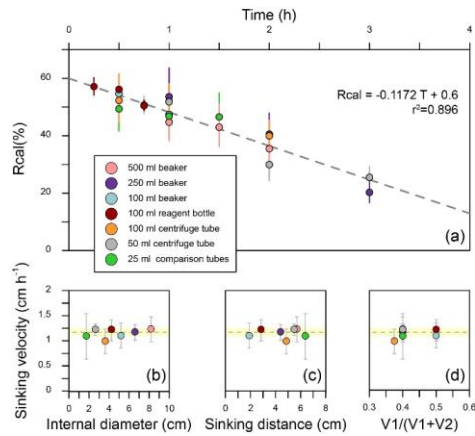
311 **Figure 3.** The shape parameters of vessels.  $V_1$  and  $V_2$  means the volume of upper suspension and lower  
 312 suspension, respectively.  $D$  means sinking distance.  $\Phi$  means average inner diameter which is  
 313 calculated by  $\frac{2 \cdot (V_1 + V_2)}{\pi D^2}$ .

Formatted: Subscript  
 Formatted: Subscript  
 Formatted: Subscript  
 Formatted: Superscript



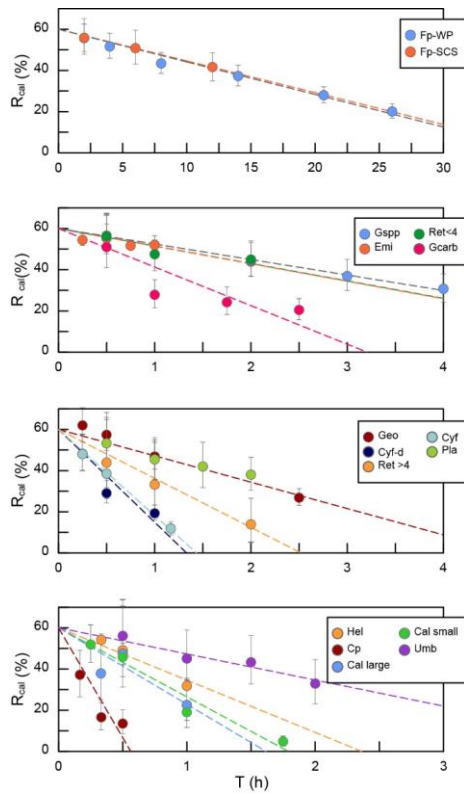
314  
 315

316 **Figure 4.** Sinking velocities of *G. oceanica* in the core KX-21-2 measured in different vessels. (a) The  
 317 calibrated separation ratios measured in different vessels. Error bars show 95% confidence level of  
 318 calibrated separation ratio. (b-d) The relationship between sinking velocity and different vessel shape  
 319 parameters. Error bars represent 95% confidence level of sinking velocity in each vessel and the shade  
 320 area represents 95% confidence level of sinking velocity considering all data points.



321

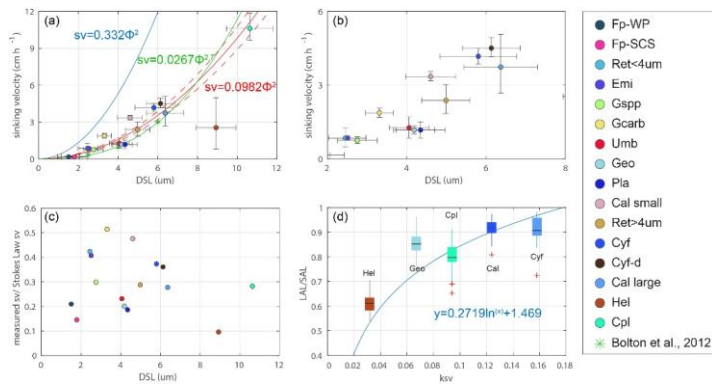
322 **Figure 5.** The calculated separation ratio (R<sub>cal</sub>) vs sinking duration. Fp-WP means *F. profunda* in the  
 323 West Pacific. Fp-SCS means *F. profunda* in the South China Sea. Emi means *E. huxleyi*. Gsp means  
 324 small *Geophycapsa*. Geo means *G. oceanica*. Gcarb means *G. caribbeanica*. Ret<4 means small  
 325 *Reticulofenestra*. Ret>4 means large *Reticulofenestra*. Cyf means *Cyclicargolithus floridanus*. Cy-d  
 326 means dissolved *Cy. floridanus*. Umb means *U. sibogae*. Pla means *Pseudoemiliania*  
 327 *lacunose*/*lacunosa*. Hel means *Helicosphaera*/*H. carteri*. Cal large means larger *Calcidiscus*  
 328 *leptopus*. Cal small means small *Ca. leptopus*. Cpl means *Co. pelagicus*.



329  
 330

331

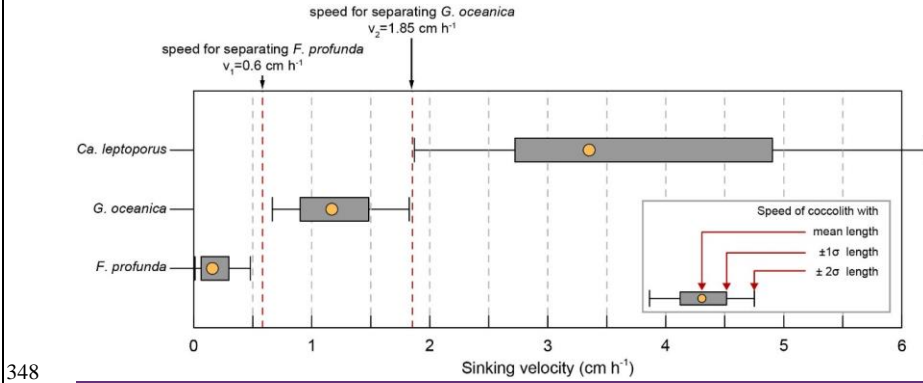
332 **Figure 6.** Coccolith sinking velocities and coccolith shape factors. (a-b) Sinking velocities and mean  
333 distal shield length. The horizontal error bars represent one standard deviation of coccolith length and  
334 the vertical ones represent 95% confidence level of measured sinking velocities. The blue, green and  
335 red lines represent sinking velocity of calcite sphere objects, coccolith sinking velocities estimated by  
336 Bolton et al. (2012) and this study, respectively. (c) The ratio of measured speed and speed calculated  
337 by Stokes' Law. (d) Coccolith short axis length (SAL) and long axis length (LAL) ratio against shape-  
338 velocity factor  $k_{sv}$ . Box shows median value and upper/lower quartiles, whiskers show maximum and  
339 minimum values, outliers larger than 1.5 of the interquartile range are shown as red crosses. The SAL  
340 against LAL plot was shown in Figure C3. The short names of coccoliths can be found in Table 2.



341

342

343 **Figure 7.** The selection of separation velocities: the sinking velocities of three main coccolith species  
 344 in sample from core KX21-2 were calculated by the length distribution and velocity factors in Table 2.  
 345 The yellow dots represent sinking velocities of coccoliths with mean length. The edge of boxes show  
 346 the sinking velocities of coccolith within one standard deviation of length ( $\pm 1\sigma$ ) and the whiskers  
 347 mark the sinking velocities of coccolith within two standard deviation of length ( $\pm 2\sigma$ ).



348

**Formatted:** Font: Bold  
**Formatted:** Check spelling and grammar

**Formatted:** German (Switzerland)  
**Formatted:** Normal

349 **References**

- 350 Bach, L.T., Riebesell, U., Sett, S., Febiri, S., Rzepka, P., Schulz, K.G., 2012. An approach for  
351 particle sinking velocity measurements in the 3-400  $\mu\text{m}$  size range and considerations on  
352 the effect of temperature on sinking rates. *Mar Biol* 159, 1853-1864, doi:10.1007/s00227-  
353 012-1945-2.
- 354 Barnea, E., Mizrahi, J., 1973. A generalized approach to the fluid dynamics of particulate  
355 systems: Part 1. General correlation for fluidization and sedimentation in solid  
356 multiparticle systems. *The Chemical Engineering Journal* 5, 171-189, doi:10.1016/0300-  
357 9467(73)80008-5.
- 358 Baumann, K.-H., 2004. Importance of size measurements for coccolith carbonate flux estimates.  
359 *Micropaleontology*, 35-43.
- 360 Beaufort, L., Lancelot, Y., Camberlin, P., Cayre, O., Vincent, E., Bassinot, F., Labeyrie, L.,  
361 1997. Insolation cycles as a major control of equatorial Indian Ocean primary production.  
362 *Science* 278, 1451-1454, doi:10.1126/science.278.5342.1451.
- 363 Beltran, C., de Rafélis, M., Minoletti, F., Renard, M., Sicre, M.A., Ezat, U., 2007. Coccolith  
364  $\delta^{18}\text{O}$  and alkenone records in middle Pliocene orbitally controlled deposits: High-  
365 frequency temperature and salinity variations of sea surface water. *Geochemistry,*  
366 *Geophysics, Geosystems* 8, Q05003, doi:10.1029/2006GC001483.
- 367 Bolton, C.T., Hernandez-Sanchez, M.T., Fuertes, M.A., Gonzalez-Lemos, S., Abrevaya, L.,  
368 Mendez-Vicente, A., Flores, J.A., Probert, I., Giosan, L., Johnson, J., Stoll, H.M., 2016.  
369 Decrease in coccolithophore calcification and  $\text{CO}_2$  since the middle Miocene. *Nat*  
370 *Commun* 7, 10284, doi:10.1038/ncomms10284.
- 371 Bolton, C.T., Stoll, H.M., 2013. Late Miocene threshold response of marine algae to carbon  
372 dioxide limitation. *Nature* 500, 558-562, doi:10.1038/nature12448.
- 373 Bolton, C.T., Stoll, H.M., Mendez-Vicente, A., 2012. Vital effects in coccolith calcite:  
374 Cenozoic climate- $\text{pCO}_2$ drove the diversity of carbon acquisition strategies in  
375 coccolithophores, *Paleoceanography* 27, doi:10.1029/2012pa002339.
- 376 Bordiga, M., Bartol, M., Henderiks, J., 2015. Absolute nannofossil abundance estimates:  
377 Quantifying the pros and cons of different techniques. *Revue de micropaléontologie* 58,

378 155-165 doi:10.1016/j.revmic.2015.05.002.

379 Candelier, Y., Minoletti, F., Probert, I., Hermoso, M., 2013. Temperature dependence of  
380 oxygen isotope fractionation in coccolith calcite: A culture and core top calibration of the  
381 genus *Calcidiscus*. *Geochimica et Cosmochimica Acta* 100, 264-281,  
382 doi:10.1016/j.gca.2012.09.040.

383 Hermoso, M., Candelier, Y., Browning, T.J., Minoletti, F., 2015. Environmental control of the  
384 isotopic composition of subfossil coccolith calcite: Are laboratory culture data transferable  
385 to the natural environment? *GeoResJ* 7, 35-42, doi:10.1016/j.grj.2015.05.002.

386 Hermoso, M., Chan, I.Z.X., McClelland, H.L.O., Heureux, A.M.C., Rickaby, R.E.M., 2016.  
387 Vanishing coccolith vital effects with alleviated carbon limitation. *Biogeosciences* 13,  
388 301-312, doi:10.5194/bg-13-301-2016.

389 Jin, X., Liu, C., Poulton, A.J., Dai, M., Guo, X., 2016. Coccolithophore responses to  
390 environmental variability in the South China Sea: species composition and calcite content.  
391 *Biogeosciences* 13, 4843-4861, doi: 10.5194/bg-13-4843-2016.

392 Kell, G.S., 1975. Density, thermal expansivity, and compressibility of liquid water from 0. deg.  
393 to 150. deg.. correlations and tables for atmospheric pressure and saturation reviewed and  
394 expressed on 1968 temperature scale. *Journal of Chemical and Engineering Data* 20, 97-  
395 105.

396 Kestin, J., Sokolov, M., Wakeham, W.A., 1978. Viscosity of liquid water in the range -8 °C to  
397 150 °C. *Journal of Physical and Chemical Reference Data* 7, 941-948.

398 Koch, C., Young, J., 2007. A simple weighing and dilution technique for determining absolute  
399 abundances of coccoliths from sediment samples. *J. Nanoplankton Res.*

400 McClelland, H.L., Bruggeman, J., Hermoso, M., Rickaby, R.E., 2017. The origin of carbon  
401 isotope vital effects in coccolith calcite. *Nat Commun* 8, 14511,  
402 doi:10.1038/ncomms14511.

403 McClelland, H.L., Barbarin, N., Beaufort, L., Hermoso, M., Ferretti, P., Greaves, M., Rickaby,  
404 R.E.M., 2016. Calcification response of a key phytoplankton family to millennial-scale  
405 environmental change. *Scientific Reports* 6, 34263, doi: 10.1038/srep34263.

406 McNown, John S., and Jamil Malaika. "Effects of particle shape on settling velocity at low

407 Reynolds numbers." *Eos, Transactions American Geophysical Union* 31.1 (1950): 74-82.

408 Miklasz, K.A., Denny, M.W., 2010. Diatom sinkings speeds: Improved predictions and insight  
409 from a modified Stokes' law. *Limnology and Oceanography* 55, 2513-2525,  
410 doi:10.4319/lo.2010.55.6.2513.

411 Minoletti, F., Hermoso, M., Gressier, V., ~~2008~~2009. Separation of sedimentary micron-sized  
412 particles for palaeoceanography and calcareous nannoplankton biogeochemistry. *Nat.*  
413 *Protocols* 4, 14-24, doi:10.1038/nprot.2008.200.

414 Paull, C.K., Thierstein, H.R., 1987. Stable isotopic fractionation among particles in Quaternary  
415 coccolith-sized deep-sea sediments. *Paleoceanography* 2, 423-429,  
416 doi:10.1029/PA002i004p00423.

417 Edwards, A.R., 1963. A preparation technique for calcareous nannoplankton.  
418 *Micropaleontology* 9, 103-104.

419 Richardson, J., Zaki, W., 1954. The sedimentation of a suspension of uniform spheres under  
420 conditions of viscous flow. *Chemical Engineering Science* 3, 65-73.

421 Rickaby, R.E.M., Henderiks, J., Young, J.N., 2010. Perturbing phytoplankton: response and  
422 isotopic fractionation with changing carbonate chemistry in two coccolithophore species.  
423 *Clim. Past* 6, 771-785, doi:10.5194/cp-6-771-2010.

424 Rousselle, G., Beltran, C., Sicre, M.-A., Raffi, I., De Raféllis, M., 2013. Changes in sea-surface  
425 conditions in the Equatorial Pacific during the middle Miocene–Pliocene as inferred from  
426 coccolith geochemistry. *Earth and Planetary Science Letters* 361, 412-421,  
427 doi:10.1016/j.epsl.2012.11.003.

428 Sprengel, C., Baumann, K.-H., Henderiks, J., Henrich, R., Neuer, S., 2002. Modern  
429 coccolithophore and carbonate sedimentation along a productivity gradient in the Canary  
430 Islands region: seasonal export production and surface accumulation rates. *Deep Sea*  
431 *Research Part II: Topical Studies in Oceanography* 49, 3577-3598 doi: 10.1016/S0967-  
432 0645(02)00099-1.

433 Stoll, H.M., 2005. Limited range of interspecific vital effects in coccolith stable isotopic records  
434 during the Paleocene-Eocene thermal maximum. *Paleoceanography* 20,  
435 doi:10.1029/2004pa001046.



436 Stoll, H.M., Rosenthal, Y., Falkowski, P., 2002. Climate proxies from Sr/Ca of coccolith calcite:  
437 calibrations from continuous culture of *Emiliana huxleyi*. *Geochimica et Cosmochimica*  
438 *Acta* 66, 927-936, doi:10.1016/S0016-7037(01)00836-5.

439 Stoll, H.M., Ziveri, P., 2002. Separation of monospecific and restricted coccolith assemblages  
440 from sediments using differential settling velocity. *Marine Micropaleontology* 46, 209-  
441 221, doi: 10.1016/S0377-8398(02)00040-3.

442 [Tremblin, M., Hermoso, M., Minoletti, F., 2016. Equatorial heat accumulation as a long term](#)  
443 [trigger of permanent Antarctic ice sheets during the Cenozoic. \*Proceedings of the National\*](#)  
444 [Academy of Sciences 113, 11782-11787 doi: 10.1073/pnas.1608100113.](#)

445 Xie, H-Y., and D-W. Zhang. "Stokes shape factor and its application in the measurement of  
446 sphericity of non-spherical particles." *Powder Technology* 114.1 (2001): 102-105 doi:  
447 10.1016/S0032-5910(00)00269-2.

448 Young, J.R., Ziveri, P., 2000. Calculation of coccolith volume and its use in calibration of  
449 carbonate flux estimates. *Deep sea research Part II: Topical studies in oceanography* 47,  
450 1679-1700, doi:10.1016/S0967-0645(00)00003-5.

451 Zhang, H., Liu, C., Jin, X., Shi, J., Zhao, S., Jian, Z., 2016. Dynamics of primary productivity  
452 in the northern South China Sea over the past 24,000 years. *Geochemistry, Geophysics,*  
453 *Geosystems* 17, 4878-4891, doi:10.1002/2016GC006602 .

454 Ziveri, P., Stoll, H., Probert, I., Klaas, C., Geisen, M., Ganssen, G., Young, J., 2003. Stable  
455 isotope 'vital effects' in coccolith calcite. *Earth and Planetary Science Letters* 210, 137-  
456 149, doi:10.1016/S0012-821X(03)00101-8.

457 **Appendix A. Sample selections**

458 **Table A1.** Sample selections

Measured coccolith	abb.	Region	Core	Section	Epoch	Age model ref.
<i>F. profunda</i>	Fp-SCS	SCS	MD12-3428	0-1 cm	Holocene	Zhang et al., 2016
<i>F. profunda</i>	Fp-WP	W.P.	KX21-2	2-4 cm	Holocene	Liang et al., 2016
<i>E. huxleyi</i>	Emi	SCS	MD12-3428	0-1 cm	Holocene	Zhang et al., 2016
<i>Gephyocapsa</i> spp.	Gspp	W.P.	ODP 807A	1H 5W 102-104	Pleistocene	Jin et al., 2010
<i>G. oceanica</i>	Geo	W.P.	KX21-2	2-4 cm	Holocene	Liang et al., 2016
<i>G. caribbeanica</i>	Gcarb	N.A.	IODP 1304B	7H 5W 69-70	Pleistocene	Channell et al., 2010
small <i>Reticulofenestra</i>	Ret<4	SCS	IODP 1433B	28R 2W 30-34	Miocene	Li et al., 2013
large <i>Reticulofenestra</i>	Ret>4	SCS	IODP 1433B	28R 2W 30-34	Miocene	Li et al., 2013
<i>Cyclicargolithus floridanus</i>	Cyf	SCS	IODP 1435A	6R 3W 25-29	Oligocene	Li et al., 2013
<i>Cyclicargolithus floridanus</i>	Cyf-d	SCS	IODP 1435A	8R 1W 27-31	Oligocene	Li et al., 2013
<i>Umbilicosphaera sibogae</i>	Umb	W.P.	ODP 807A	3H 5W 92-94	Pleistocene	Jin et al., 2010
<i>Pseudoemiliana lacunosa</i>	Pla	W.P.	ODP 807A	3H 5W 92-94	Pleistocene	Jin et al., 2010
<i>Helicosphaera carteri</i>	Hel	W.P.	ODP 807A	3H 5W 92-94	Pleistocene	Jin et al., 2010
large <i>Calcidiscus leptoporus</i>	Cal large	W.P.	ODP 807A	3H 5W 92-94	Pleistocene	Jin et al., 2010
small <i>Calcidiscus leptoporus</i>	Cal small	N.A.	IODP 1304B	7H 5W 69-70	Pleistocene	Channell et al., 2010
<i>Coccolithus pelagicus</i>	Cpl	N.A.	IODP 1304B	7H 5W 69-70	Pleistocene	Channell et al., 2010

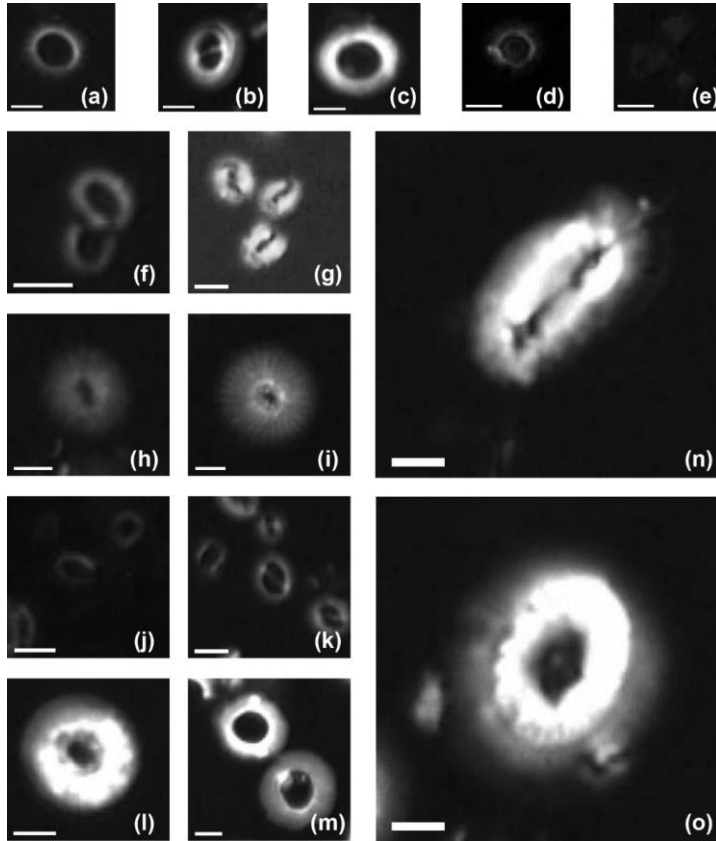
459

460 **References:**

- 461 Channell, J., Sato, T., Kanamatsu, T., Stein, R., Alvarez Zarikian, C., 2010. Expedition  
462 303/306 synthesis: North Atlantic climate. Channell, JET, Kanamatsu, T., Sato, T., Stein,  
463 R., Alvarez Zarikian, CA, Malone, MJ, and the Expedition 303, 306.  
464 Jin, H., Jian, Z., Cheng, X., Guo, J., 2011. Early Pleistocene formation of the asymmetric  
465 east-west pattern of upper water structure in the equatorial Pacific Ocean. Chinese  
466 Science Bulletin 56, 2251-2257.

- 467 Li, C.-F., Lin, J., Kulhanek, D.K., 2013. South China Sea tectonics: Opening of the South  
468 China Sea and its implications for southeastAsian tectonics, climates, and deep mantle  
469 processes since the late Mesozoic. IODP Sci. Prosp 349.
- 470 Liang, D., Liu, C., 2016. Variations and controlling factors of the coccolith weight in the  
471 Western Pacific Warm Pool over the last 200 ka. Journal of Ocean University of China  
472 15, 456-464.
- 473 Zhang, H., Liu, C., Jin, X., Shi, J., Zhao, S., Jian, Z., 2016. Dynamics of primary productivity  
474 in the northern South China Sea over the past 24,000 years. Geochemistry, Geophysics,  
475 Geosystems 17, 4878-4891.

476 **Appendix B. Coccolith images under circular polarized light**

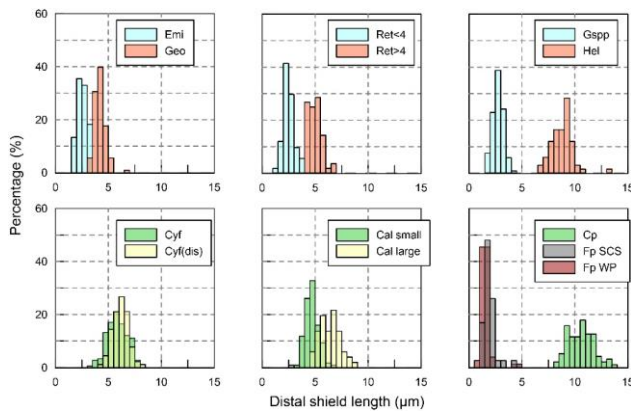


477  
 478 **Plate B1.** Imaged of measured coccolith in this study: (a) *Pseudoemiliana lacinosa* in the core ODP  
 479 807; (b) *Gephyrocapsa oceanica* in the core KX21-2; (c) *Reticulofenestra* spp. (large) in the core  
 480 IODP U1433B; (d) *Umbilicosphaera sibogae* in the core ODP 807; (e) *Florispharea profunda* in  
 481 the core KX21-2; (f) *Reticulofenestra* spp. (small) in the core IODP U1433B; (g) *Gephyrocapsa*  
 482 *caribbeanica* in the core IODP U1304B; (h) small *Calcidiscus leptoporus* in the core IODP  
 483 U1304B; (i) large *Calcidiscus leptoporus* in the core ODP 807A; (j) *Emiliana huxleyi*  
 484 in the surface sediment in the South China Sea; (k) *Gephyrocapsa* spp. in the core ODP 807; (l)  
 485 *Cyclicargolithus floridanus* in the core IODP U1435A and (m) dissolved *Cyclicargolithus*  
 486 *floridanus* in the same core; (n) *Helicosphaera carteri* in the core ODP 807A; (o) *Coccolithus*  
 487 *pelagicus* in the core IODP U1304B. White bars represent a length of 2  $\mu$ m.

Formatted: Font: Italic

488 **Appendix C. The length distribution of coccoliths**

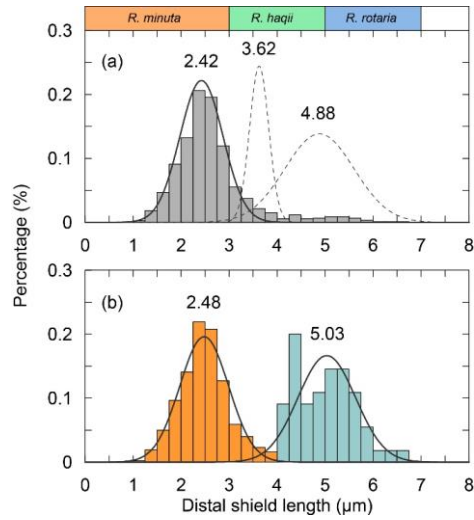
489 To measure the distal shield length of coccoliths, pictures were taken at a magnification of 1250x  
 490 under circular polarized light. The coccolith lengths were measured by using the image analysis  
 491 software, ImageJ. More than 5 pictures were taken and more than 50 (usually more than 100)  
 492 coccolith specimens were measured. The length distributions of coccoliths measured in our  
 493 experiments were shown in the Figure C1.



494

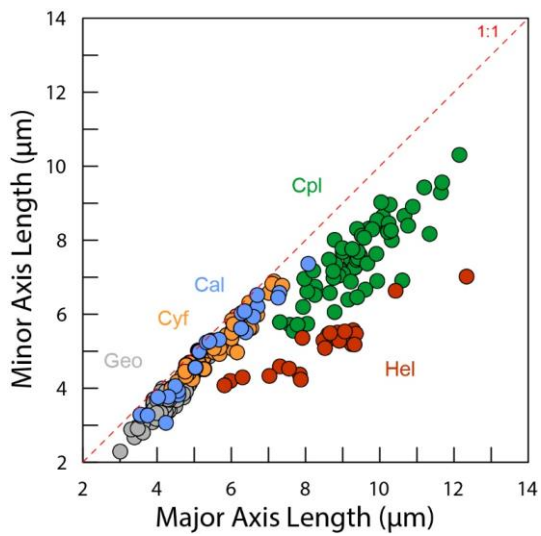
495 **Figure C1.** Size distribution of coccolith measured in the present study. The shorten names of coccolith  
 496 follow Table A1.

497 The classification of coccoliths by length was supported by mixture analysis in PAST (Hammer et  
 498 al., 2001), such as *Reticulofenestra* spp. and *Gephyrocapsa* spp. *Reticulofenestra* spp. in the  
 499 Miocene were classified into two groups, Ret. (<4 µm) and Ret. (>4 µm). The traditional  
 500 classification of *Reticulofenestra* spp. is <3 µm, 3-5 µm and 5-7 µm didn't pass the normal  
 501 distribution test. Hence, in this study the *Reticulofenestra* spp. are divided at 4 µm (Figure C2).  
 502 *Gephyrocapsa* spp. were classified by the shape of coccoliths into small *Gephyrocapsa* (central area  
 503 opening and length <3.5 µm), *G. oceanica* (central area opening and length >3.5µm) and *G.*  
 504 *caribbeanica* (closed central area) by the length and central area.



505

506 **Figure C2.** The classical classification of *Reticulofenestra* spp. (a) and the classification used in our  
 507 study (b). The curves represent the normal distribution fits of different coccolith groups and the dish  
 508 curve marks that the goodness of fit is below 0.2.



509

510 **Figure C3.** The short axis and long axis length distribution of coccoliths in Figure 6d.

511 **Reference.**

512 Hammer, Ø., Harper, D., Ryan, P., 2001. Paleontological Statistics Software: Package for  
513 Education and Data Analysis. Palaeontologia Electronica.

Formatted: English (United States)

514 **Appendix D. Coccolith movement in gravity settling**

515 In this part, the derivation of equation will be explained in detail including proofs of several  
 516 assumptions mentioned in the methods part.

517  
 518 When the well mixed sediment begins to sink, the decrease of coccoliths number in the upper  
 519 suspension ( $N_u$ ) can be described as following equation:

520 
$$\frac{dN_u}{dt} = -\frac{N_u(t=0)}{D} \times sv \quad (D-1)$$

521 where the D is the length of upper suspension and  $N_{u(t=0)} / D$  is the initial number of coccolith in  
 522 cross-section with a unit thickness of  $dD$ ,  $v$  is the sinking velocity of coccolith.

523 Do integration for the equation D-1, we can get the variation of coccolith number in the upper  
 524 column over time:

525 
$$N_u = N_{u(t=0)} - \frac{N_{u(t=0)}}{D} \times sv \times T \quad (D-2)$$

526 where T is settling time. After a period of time (T), we pump out the upper suspension. Here we  
 527 define the number of coccoliths in the upper supernatant dividing the total coccoliths number in the  
 528 tube ( $N_t$ ) as separation ratio (R), which represents the percentage of total coccoliths removed in one  
 529 separation. This parameter is important and will be repeatedly mentioned in the following part. R  
 530 can be expressed by

531 
$$R = \frac{N_u}{N_t} \quad (D-3)$$

532 Assuming all coccoliths are uniformly distributed in the suspension at the beginning of settling,

533  $N_{u(t=0)}$  has relationship with  $N_t$  as follow:

534 
$$\frac{N_u(t=0)}{N_t} = \frac{V_1 V_1}{V_1 V_1 + V_2 V_2} \quad (D-4)$$

535 where  $V_1$  is the volume of upper suspensions and  $V_2$  is the volume of lower suspensions.

536 Combining the equation D-1, D-2, D-3 and D-4, we obtain the relationship between separation ratio,  
 537 R, and sinking velocity,  $sv$ , as follow:

538 
$$R = \frac{N_u}{N_t} = \frac{N_{u(t=0)} - \frac{N_{u(t=0)}}{D} \times sv \times T}{N_t} = \frac{V_1 - \frac{V_1}{D} \times sv \times T}{V_1 + V_2} \quad (D-5)$$

539 If we plot the R and T on a figure, the slope of the line is a function of  $V_1$ ,  $V_2$ , D and  $sv$ . Since the  
 540  $V_1$ ,  $V_2$ , D are known parameters, we say the slope of R-T is a function of  $sv$ , which is exactly what  
 541 we want.

Formatted: Subscript

Formatted: Subscript

Formatted: Subscript

Formatted: Subscript

Formatted: Subscript

Formatted: Subscript

Formatted: Subscript

Formatted: Subscript

Formatted: Subscript



542 Comparison tubes used in our experiments have the same  $V_1$  and  $V_2$  but different D. Other vessels  
 543 used in other experiments have different  $V_1$ ,  $V_2$  and D. So we should adjust the raw separation ratio  
 544 to calibrated separation ratio ( $R_{cal}$ ), which represents the separation ratio made in a standard vessel  
 545 with  $V_{1std}=15$  ml,  $V_{2std}=10$  ml and  $D_{std}=6$  cm. This step can be described by equation D-6:

$$R_{cal} = \frac{[R \times (V_1 V_2 + V_1 V_2) - V_1 V_2] \times D \times V_{1std}}{(D_{std} \times V_1 V_2 + V_{1std}) \times (V_{1std} + V_{2std})} \quad (D-6)$$

547 After calibrated, the slope of  $R_{cal}$ -T (k) has relationship with  $SV$  as following equation:

$$SV = -\frac{D_{std} \times (V_{1std} + V_{2std})}{V_{1std}} \times k = -10 \times k \quad (D-7)$$

549 where k is the slope of  $R_{cal}$  against T from regression and other parameters are as described above.

550 Hence, the sinking velocity of different coccoliths can be achieved by measuring the variations of  
 551  $R_{cal}$  over time.

552 The coccoliths' lengths in the sediment have some variations. So what we measured is actually the  
 553 bulk settling velocity of whole coccolith population. We also offer a test for the assumption that the  
 554 average sinking velocity of all coccoliths can be treated as the sinking velocity of coccoliths with  
 555 the average length. Here we used the data of *G. oceanica*. A normal distribution was fitted to the  
 556 measured length distribution (Figure D1-a). We generated 100000 coccolith following the normal  
 557 distribution and let these coccolith evenly distributing in the comparison tube at the initial and then  
 558 set them sinking without collisions with each other. And then we simulate a normal distribution  
 559 situation of coccoliths in the vessel. The sinking velocities of different size coccoliths were  
 560 calculated by the cubic-velocity-shape parameter ' $b^2 k_v$ ' as described in discussion part. We modeled  
 561 the coccoliths sinking process and computed the separation ratio (red dash line in Figure D1-b),  
 562 coccolith length (red dash line in Figure D1-c) and instant sinking velocities (orange dots in Figure  
 563 D1-d) at different time sections.

Formatted: Subscript

Formatted: Subscript

Formatted: Subscript

Formatted: Subscript

Formatted: Subscript

Formatted: Subscript

Formatted: Subscript

Formatted: Subscript

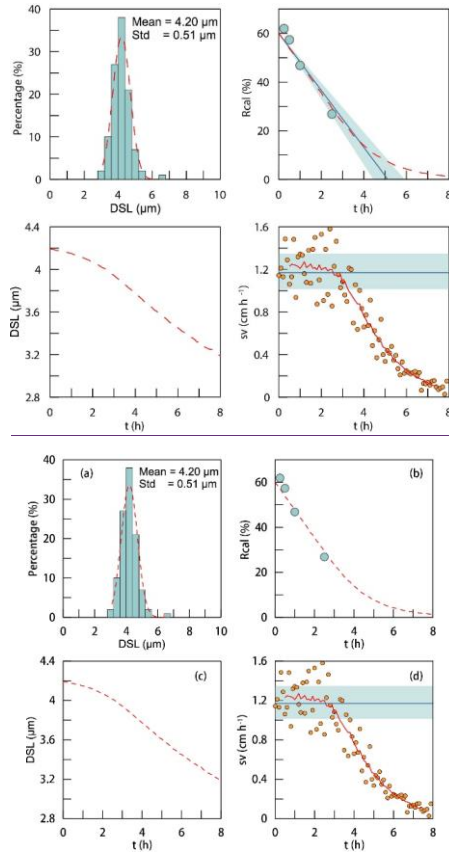
Formatted: Subscript

Formatted: Subscript

Formatted: Subscript

Formatted: Font: Italic

Formatted: Subscript



564

565

566 **Figure D1.** The simulations of coccoliths settling with different lengths: (a) the length distribution of  
 567 coccoliths. The green bars represent measured data and red dash line represents the best fit for normal  
 568 distribution. (b) The calibrated separation ratio: the green dots are measured data in our settling  
 569 experiments, the blue line and shade area represent the calculated sinking velocity based on  $R_{cal}$   
 570 measurement and the red dash line represents results obtained from Monte Carlo simulations. (c) The  
 571 average length of removed coccolith in simulations; (d) the modeling sinking velocities of coccoliths:  
 572 the orange dots are instant sinking velocity calculated from derivation of  $R_{cal}$ , the red dash line is  
 573 weighted average for the instant sinking velocity. Blue line represents the average sinking velocity we  
 574 measured and the green shade area represents 95% confidence level of the measured velocity.

575 For *G. oceanica* experiments, the instant sinking velocity would not change significantly until  
 576 settling for more 3 hours. That means for all  $R_{cal}$  larger than 15% are safe for liner regressions. The

Formatted: Font: (Default) Times New Roman, (Asian) Times New Roman

Formatted: Subscript

Formatted: Subscript

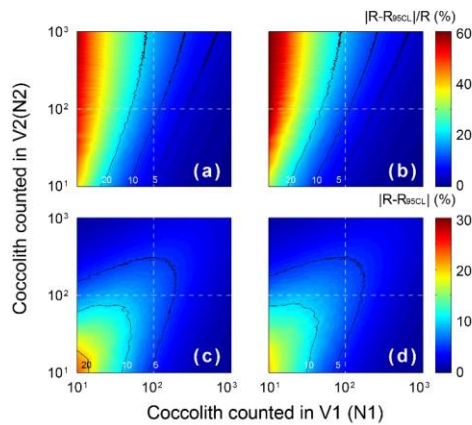
Formatted: Subscript

577 minimum safe number of  $R_{\text{gal}}$  will descend with the drop of dispersion degree of coccolith length  
578 distribution. Hence our assumption for average sinking velocity and the use of liner regression are  
579 proved to be reasonable.

**Formatted:** Subscript

580 **Appendix E. Statistical and error analyses**

581 The errors of measured separation ratio (R) and calculated sinking velocity ( $v$ ) are mainly caused  
 582 by counting coccolith, the error of which follows the Poisson distribution. To detect the influence of  
 583 counting number on the result error, the error of separation ratio was simulated by 5000 times Monte  
 584 Carlo calculations with assumptions that ' $V_1:V_2=15:10$ ' and ' $n_1=n_2$ ' (Figure E1). The result shows  
 585 that the number of coccolith counted in the upper column draws more influence on the relative error  
 586 ( $|R-R_{95CL}|/R$ ). That means more coccolith in the upper suspension should be counted to make results  
 587 more accurate. The slope of  $R_{cal}-T$  was calculated by liner fitting with the intercept fixed on  
 588  $V_1/(V_1+V_2)$ . The input  $R_{cal}$  were generated from measured values considering the error of coccolith  
 589 counting. The error of sinking velocity regressions of  $R_{cal}-T$  was also were repeated —calculated by  
 590 5000 times Monte Carlo simulations regressions in the software Matlab and the error of sinking  
 591 velocity,  $v$ , was source from the distribution slope of  $R_{cal}-T$  in Monte Carlo process.—



592  
 593 **Figure E1.** The error distribution with different  $N_1$  and  $N_2$  (ranging from 1 to 1000) simulated 5000  
 594 times by the Matlab with assumptions that the error distributions of  $N_1$  and  $N_2$  fellow Poisson  
 595 distribution. The calculation of R follows equation 2-5, and here we assume numbers of FOV are equal  
 596 ( $n_1=n_2$ ). Counter lines mark values equal to 5, 10 and 20. (a) and (c) represent the lower 95%  
 597 confidence level and (b) and (d) represent upper 95% confidence level. (a) and (b) the relative error of  
 598 R and (c) and (d) represent the absolute error of R.

Formatted: Subscript  
 Formatted: Subscript  
 Formatted: Subscript  
 Formatted: Subscript  
 Formatted: Subscript  
 Formatted: Subscript  
 Formatted: Subscript  
 Formatted: Subscript  
 Formatted: Subscript  
 Formatted: Subscript  
 Formatted: Subscript

Formatted: Subscript  
 Formatted: Subscript  
 Formatted: Subscript  
 Formatted: Subscript  
 Formatted: Subscript  
 Formatted: Subscript